Turkish Journal of Electrical Engineering & Computer Sciences

http://journals.tubitak.gov.tr/elektrik/

Research Article

Turk J Elec Eng & Comp Sci
(2017) 25: 3037 – 3051

doi:10.3906/elk-1609-75

A bidirectional wireless power transfer system for an electric vehicle with a relay circuit

Chenyang XIA, Wei WANG*, Yuling LIU, Kezhang LIN, Yanhe WANG, Xiaojie WU
School of Information & Electrical Engineering, Faculty of Electrical Engineering,
China University of Mining and Technology, Xuzhou, P.R. China

Received: 09.09.2016 • **Accepted/Published Online:** 26.11.2016 • **Final Version:** 30.07.2017

Abstract: In order to extend the transfer distance, enhance the tolerance for coil misalignment, and improve the capability of energy feedback and power transfer efficiency of conventional wireless power transfer (WPT) systems for electric vehicles, this paper presents a bidirectional WPT topology with a relay circuit. In the proposed topology, the primary and pickup circuits are implemented with virtually identical structures, which can operate in both magnetic field excitation and magnetic field receiving modes to facilitate bidirectional power flow between the primary side and the pickup side. A relay circuit is introduced to achieve high transfer efficiency under special conditions such as long distance or coil misalignment. The mathematical model of the system is established to describe its working mechanism in detail. Both the direction and amount of power flow can be regulated by controlling the shift phase voltages generated by primary and pickup switches. At the same time, the power and efficiency of system are analyzed, which provides a reference to optimize the parameters. The viability of the proposed system is verified by experiments, and the results suggest that the relay bidirectional WPT system is a reliable and efficient system for electric vehicle charging systems.

Key words: Wireless power transfer, electric vehicle, relay, bidirectional power transfer

1. Introduction

The wireless power transfer (WPT) system based on the inductive coupled power transfer (ICPT) technique can transmit electric energy from the power sources to the loads without any wires between the two sides, which offers advantages in terms of flexibility, reliability, and safety [1–4]. Therefore, it has been gaining popularity and is widely used in some special fields, including household appliances, implanted biomedical sensors for organs, underwater charging, and online electric power supply [5–8]. The development trend of WPT technology is long-distance, high-power, high-efficiency, misalignment-tolerant, etc. [9–11].

WPT technology is a contactless power transfer method using magnetic field coupling, and therefore the distance of transfer should be as long as possible to make WPT technology widely used in industrial and household applications. To realize quick charging in some applications, e.g., electric vehicles (EVs), WPT systems used in these applications should have the feature of high-power transfer. Due to the application of high-frequency converters and the existence of ESRs of coils in WPT systems, it is necessary to study the improvement of efficiency of WPT systems. Coil misalignment is a common problem in WPT systems, as it can lead to the fluctuation of transferred power. Therefore, a WPT system with tolerance of misalignment is investigated in terms of circuit topology, magnetic structure, and control methods.

*Correspondence: cumtsieeww@126.com

With the rapid development of new energy vehicles, wireless charging systems for EVs have received much attention. The structure of a typical wireless charging system for EVs is shown in Figure 1, where a wireless charging system for the EV consists of two electrically isolated parts, namely the primary side and the pickup side.

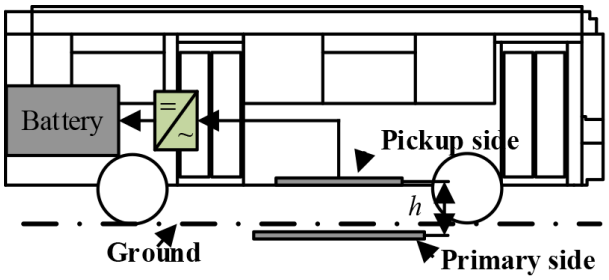

Figure 1. A typical WPT system for an electric vehicle.

At the primary side, which is usually installed under the ground, a high-frequency current is generated in the resonant tank, resulting in high-frequency electromagnetics. The primary coil, together with an inductor-capacitor-inductance (LCL) parallel resonant circuit, generates a high-frequency electromagnetic field, which is mainly installed beneath the ground.

The pickup coil is magnetically coupled to the primary coil through the electromagnetic field, and the inductive current in the pickup coil is regulated with the rectifying and filtering circuits, which are applied to charge the onboard battery pack. In general, a control circuit is included in both primary and pickup sides to adjust the charging power according to the requirements of the battery.

However, the transfer power and efficiency of the system are reduced due to factors caused by different heights of the EV chassis and parking in an inaccurate position, which have serious impacts on output power and efficiency of wireless charging systems. Besides, the WPT system has only worked in unidirectional mode such that the energy stored in the battery of the EV cannot feed back to the grid. This limitation seriously hinders the application of the WPT system in the field of EV charging. To date, scholars have done the following research on these issues:

1) Limited transfer distance: The energy transfer efficiency is decreased sharply while distance increases. At present, designers often increase the system frequency to alleviate this contradiction [12].

2) Bidirectional energy transfer: Bidirectional WPT systems have been studied in both single-phase and three-phase systems to improve the efficiency of energy feedback [13–15]. An interesting aspect of electric vehicles is the possibility of integrating the vehicle-to-grid (V2G) concept into the utility grid. In this concept, the V2G operation takes place at the moment of high demand while G2V operation happens at times of low demand.

3) The low tolerance of coil misalignment between the primary and pickup coils: To solve this problem, scholars mainly study the design of the coil [16], the impedance network, coil positioning technology, and other aspects.

In this paper, we present a new relay bidirectional mode to solve the above disadvantages for an EV WPT charging system (Figure 2). As shown in Figure 2, this system comprises three parts: the power converter and magnetic energy transmitter mechanism on the primary side, the power relay structure between the primary

and pickup sides, and the pickup coil and power conditioner on the pickup side. LCL compensation is preferably used to minimize the reactive power in the primary power converter and the pickup power conditioner. The relay structure is also an LCL resonant circuit, which relays power from the primary to the pickup. Furthermore, the relay mechanism has a flexible mechanical structure to charge the EV under conditions of long distance and coil misalignment.

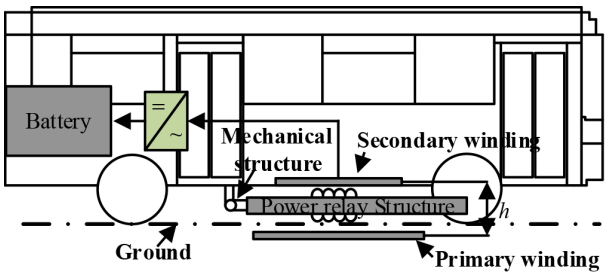

Figure 2. Schematic of the EV charging system with a relay ICPT system.

First, this paper introduces the basic structure and principle of the WPT system, and we present a novel relay bidirectional WPT system and the system topological structure. In addition, the working mode is introduced in detail. Second, the bidirectional power transfer mode and power control are researched. The shift phase control is applied to the primary and pickup, realizing the regulation of the power transmitter of the primary and received power of the load. Furthermore, the amount of the power flow and the direction can be controlled by regulating the shift phase angle. Third, to optimize the system parameters, this paper focuses on the transfer power and efficiency. Finally, the working process of the system is verified by simulation and experiment.

2. Configuration of WPT system for an electric vehicle

A typical EV WPT system is shown in Figure 1, where the structure of the primary power converter is the full bridge topology. In the WPT system, the primary and pickup coils generally have large leakage inductance, and therefore a resonant circuit is employed in the primary and pickup side system to provide the reactive power compensation, maximize the amount of power delivery, and improve the efficiency of the system. To realize the full resonant state of the system, the WPT system usually works in fixed frequency mode or variable frequency mode. However, due to different types of EV batteries, the fixed frequency control mode is more suitable for an EV WPT system. In addition, it is convenient for universal design if the current of the primary coil is constant. The LCL resonant compensation topology can work in fixed frequency and current constant mode [17]; therefore, the LCL resonant compensation network is widely used in the field of WPT.

3. Topology and model of relay WPT system for an electric vehicle

This paper proposes the relay bidirectional WPT system shown in Figure 3 to solve the problem of limited transfer distance, the low tolerance of coil misalignment, the lack of energy feedback, and the low transfer efficiency.

The proposed relay bidirectional WPT system employs a power converter and reversible magnetic energy mechanism on the primary side, the relay structure between the primary and pickup side, and a pickup power conditioner and reversible magnetic energy mechanism on the pickup side. The full bridge power converter on the primary side, which includes power switches Q_1, Q_2, Q_3, Q_4 and their respective internal diodes,

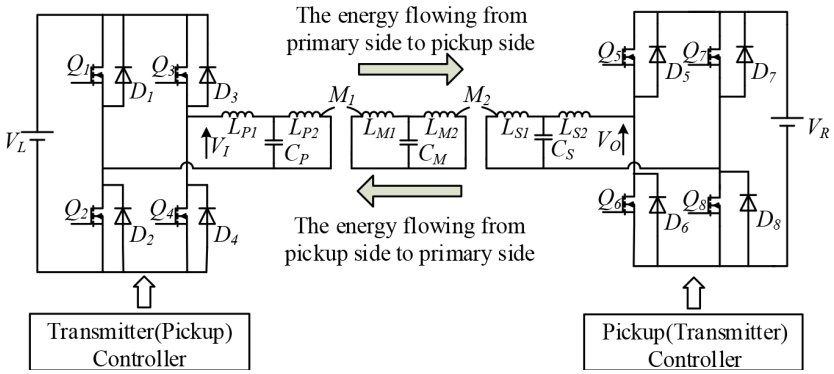

Figure 3. The circuit topology the proposed relay bidirectional WPT system.

is operated in high-frequency inverting mode. In addition, the full bridge power conditioner on the pickup side, which includes power switches Q_5, Q_6, Q_7, Q_8 and their respective internal diodes, is operated in PWM rectifying mode. The primary resonant LCL (L_{P1}, L_{P2}, and C_P) circuit generates power flow. Similarly, L_{M1}, L_{M2}, and C_M form the LCL power relay circuit to relay the power from the primary to the pickup side while the pickup LCL (L_{S1}, L_{S2}, and C_S) receives the power flow. M_1 and M_2 represent mutual inductance between the primary and the relay coil and mutual inductance between the relay and pickup coil, respectively. The primary and pickup sides have an independent control circuit that can control both the amount and direction of power flow effectively. The primary and pickup circuits are implemented with virtually identical structures, so the energy from the pickup side to the primary side will not repeat.

In the relay WPT system, the LCL magnetic mechanism can change its structure according to the actual needs due to a variable LCL relay circuit used in the system between the primary coil and pickup coils. The use of the relay mode realizes a wireless charging system for EVs efficiently, which overcomes the existing shortcomings of EV wireless charging systems:

1) The realization of long distance energy transfer: A long distance wireless charging system for EVs is shown in Figure 4. When the distance between the primary and pickup is too large, an LCL relay circuit can be automatically added between the primary and pickup coil, which can theoretically meet the demand of any distance WPT for electric vehicle.

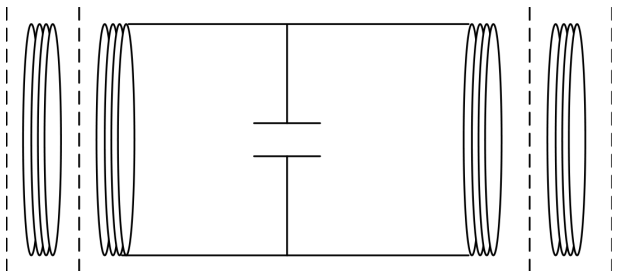

Figure 4. Long distance transfer mode.

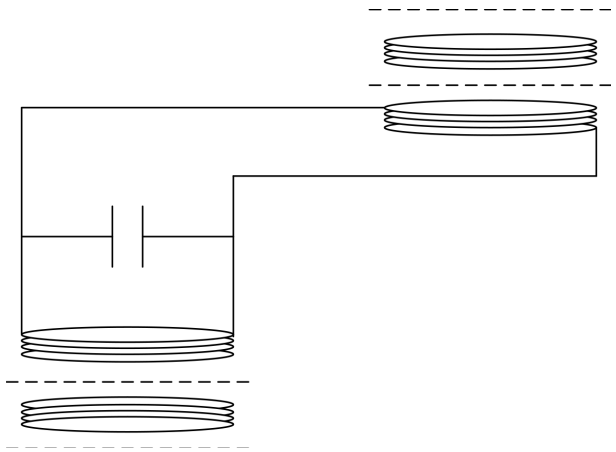

Figure 5. Energy transfer mode under conditions of coil misalignment.

2) Efficient energy transfer under conditions of coil misalignment: Figure 5 shows the energy transfer mode under the condition of coil misalignment. As shown in Figure 5, theoretically, the system can meet the demand of WPT for EVs under any coil misalignment and any angle offset by adding a bendable LCL relay circuit between the primary and pickup sides.

3) Bidirectional energy transfer: The relay WPT system has completely symmetrical circuit topology for both the primary side and the pickup side. Therefore, both the primary and pickup can work in magnetic field excitation mode and magnetic field receiving mode in order to meet the needs of bidirectional energy transfer. The system can also regulate the amount and direction of power flow dynamically according to the working conditions.

4. Control of bidirectional power transfer for electric vehicle

4.1. Analysis of bidirectional power transfer

The proposed relay bidirectional WPT system given in Figure 3 can be simplified as the equivalent circuit shown in Figure 6, where V_I is the output voltage of the primary power converter circuit, V_N is the induced voltage of the primary transmitter coil, V_M is the induced voltage of the relay receiving coil, V_Q is the induced voltage of the relay transmitter coil, V_P is the pickup received voltage, V_O is the equivalent AC voltage of output generated by the reversible rectifier of pickup side, I_{P1} is the primary current generated by the high-frequency inverter, I_{P2} is the primary transmitter current, I_{M1} is the received current of the relay coil, I_{M2} is the relay transmitter coil current, I_{S1} is the pickup received current, and I_{S2} is the output current of the pickup circuit.

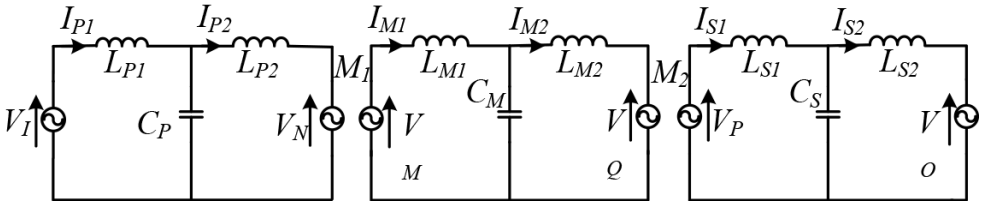

Figure 6. Steady-state model.

In a steady-state circuit, LCL circuits in the primary, relay, and pickup are fully tuned, such that

$$\frac{1}{L_{P1}C_P} = \frac{1}{L_{P2}C_P} = \frac{1}{L_{M1}C_M} = \frac{1}{L_{M2}C_M} = \frac{1}{L_{S1}C_S} = \frac{1}{L_{S2}C_S} = \omega^2, \tag{1}$$

where ω is the angular frequency of the high-frequency inverter circuit. According to the Norton equivalent principle, the primary system can be represented by the model in Figure 7.

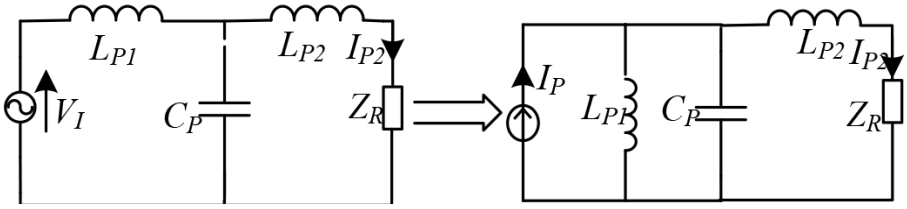

Figure 7. Primary equivalent circuit.

The primary supply generates a constant track current in L_{p2}, which is magnetically coupled to the relay

coil so that the relay circuit received voltage V_M can be represented by:

$$V_M = \omega M_1 I_{P2} = \frac{V_I M_1}{L_{P1}}. \tag{2}$$

The relay circuit transmitter current I_{M2}:

$$I_{M2} = \frac{V_M}{\omega L_{M1}} = \frac{V_I M_1}{j\omega L_{M1} L_{P1}}. \tag{3}$$

The pickup received voltage V_p:

$$V_P = \omega M_2 I_{M2} = \frac{V_I M_1 M_2}{L_{M1} L_{P1}}. \tag{4}$$

The output current of pickup received I_{s2}:

$$I_{S2} = \frac{V_P}{\omega L_{S1}} = \frac{V_I M_1 M_2}{\omega L_{S1} L_{M1} L_{P1}}. \tag{5}$$

V_I and V_O, which are assumed as the output voltage of the primary power converter and the output voltage of the pickup power conditioner, are given by:

$$V_I = |V_I| \angle \beta, V_O = |V_O| \angle \phi, \tag{6}$$

where β and φ are the initial phase angle of the output voltage of the primary power converter and the pickup power converter, respectively.

The received output power of pickup P_{out} can be calculated as:

$$P_{out} = \frac{|V_I|\,|V_O|\,M_1 M_2}{\omega L_{S1} L_{M1} L_{P1}} \sin(\beta - \phi). \tag{7}$$

From Eq. (7), it is evident that the amount and direction of power flow depends on voltage magnitudes and relative phase angles between β and φ. Thus, a leading phase ($\pi/2 \geq \beta - \varphi > 0$) constitutes the power transfer from the primary to the pickup, while a lagging phase ($0 \geq \beta - \varphi > -\pi/2$) enables power transfer from the pickup to the primary. Furthermore, the output power can be regulated by controlling the magnitude of voltage.

4.2. Shift phase voltage control of the primary side

For a given system frequency and primary inductance L_{p1}, the current of primary coil I_{P2} is only proportional to the output voltage of the primary inverter and is unaffected by load variation. This paper uses a PWM shift phase control strategy to adjust the current of primary coil I_{P2} by changing the output effective fundamental value of the inverter. Thus, the output power of the primary coil is regulated. The switch conduction time and output voltage waveform of the power converter are shown in Figure 8.

Power switches Q_1, Q_2, Q_3, and Q_4 form a full bridge in the primary as shown in Figure 3. Q_1 and Q_2 are conducted complementarily while Q_3 and Q_4 are unconducted at shift phase angle $\phi(0 \leq \phi \leq \pi)$.

The output voltage of primary power converter V_I can be expressed in Fourier terms in which $\beta(0 \leq \beta \leq 2\pi)$ is the initial phase angle of output voltage:

$$V_I = \sum_{n=1,3,5\cdots}^{+\infty} U_n \sin(n\omega t - \beta) = \sum_{n=1,3,5\cdots}^{+\infty} \frac{4V_L}{n\pi} \cos\left(\frac{n\varphi}{2}\right) \sin(n\omega t - \beta). \tag{8}$$

The output fundamental voltage is:

$$V_{I1} = \frac{4V_L}{\pi} \cos\left(\frac{\varphi}{2}\right) \sin\left(\omega t - \beta\right). \tag{9}$$

From Eq. (9), the amplitude of output fundamental voltage V_I can be regulated by changing the shift phase angle while the primary coil current I_P holds constant.

4.3. The output power of the pickup side

Figure 9 shows that the relay bidirectional WPT system applies a full bridge rectifier circuit on the pickup side. Therefore, the output voltage and direction of power flow can also be controlled by a PWM phase shift control strategy.

The phase angle of V_I with respect to V_O is assumed to be α. Thus, if the initial phase angle of the primary power converter output voltage V_I is 0, the pickup power conditioner output voltage V_O is $-\alpha$. As is evident, power is transferred from the primary to the pickup in the case above.

The output voltage of pickup power conditioner Vo can also be expressed in Fourier terms:

$$\begin{aligned} V_O &= \sum_{n=1,3,5\cdots}^{+\infty} U_n \sin\left(n\omega t + \alpha\right) \\ &= \sum_{n=1,3,5\cdots}^{+\infty} \frac{4U_O}{n\pi} \cos\left(\frac{n\lambda}{2}\right) \sin(n\omega t + \alpha) \end{aligned}. \tag{10}$$

The fundamental voltage is:

$$V_{O1} = \frac{2\sqrt{2}U_O}{\pi} \cos\left(\frac{\lambda}{2}\right) \sin\left(\omega t + \alpha\right). \tag{11}$$

The output power of the system is:

$$P_{out} = \frac{2\sqrt{2}\left|V_I\right| U_o M_1 M_2}{\pi\omega L_{S1} L_{M1} L_{P1}} \cos\left(\frac{\lambda}{2}\right) \sin\left(\alpha\right), \tag{12}$$

where λ is the shift phase angle of the pickup PWM rectifier circuit, U_o is the output voltage of the rectifier, and R_Z is the resistance load.

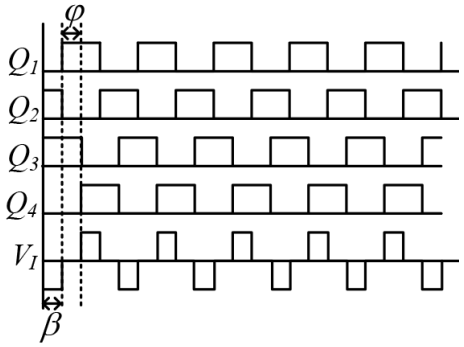

Figure 8. Switch conduction time of full bridge inverter and the output voltage.

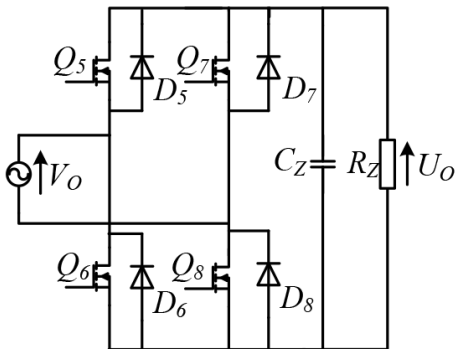

Figure 9. The output circuit of the rectifier.

Assuming that the losses of the full bridge rectifier circuit are 0, then the pickup circuit received output power is equal to the load absorbed power and thus the output voltage of rectifier bridge U_o is expressed as:

$$U_o = \sqrt{R_Z P_{out}} = \frac{2\sqrt{2}\,|V_I|\,M_1 M_2 R_Z}{\pi\omega L_{S1} L_{M1} L_{P1}} \cos\left(\frac{\lambda}{2}\right) \sin(\alpha)\,. \tag{13}$$

From Eq. (13), for a given design circuit and working frequency, the output voltage of full bridge rectifier U_o depends on shift phase angle λ, the valid values of primary power converter output voltage $|V_I|$, and the output voltage relative phase α between the primary and pickup. Furthermore, it is evident that output voltage U_o is proportional to load Rz. The output voltage can be held constant by regulating the valid output voltage of primary transmitter V_I, the shift phase angle λ, and the voltage relative initial phase α if the load varies.

5. Power and efficiency of bidirectional WPT system for EVs

The equivalent circuit is shown in Figure 10, considering the resistance of each coil.

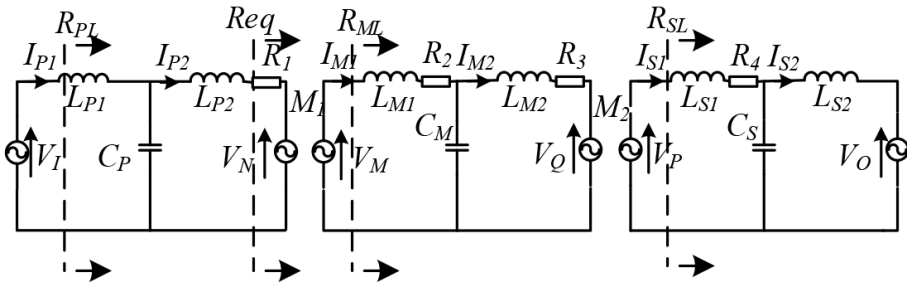

Figure 10. The equivalent circuit considering coil resistance.

R_1, R_2, R_3, and R_4 are four resistances of the mutual inductor, respectively; R_{SL} is the input equivalent resistance of the pickup; R_{ML} is the input equivalent resistance of the relay circuit; and R_{eq} is the equivalent reflected resistance of the primary.

Under conditions of system resonance, input equivalent resistance of pickup R_{SL} is:

$$R_{SL} = \frac{R_4 R_L + (\omega L_3)^2}{R_L}. \tag{14}$$

Input equivalent resistance of relay circuit R_{ML} is:

$$R_{ML} = R_2 + \frac{(\omega L_2)^2 R_{SL}}{(\omega M_2)^2 + R_{SL} R_3}. \tag{15}$$

Equivalent reflected resistance of primary R_{eq} is:

$$R_{eq} = \frac{(\omega M_1)^2}{R_{ML}}. \tag{16}$$

The current of primary coil I_{P2} is:

$$I_{P2} = \frac{V_I}{\omega L_1}. \tag{17}$$

The induced voltage of the relay circuit that is magnetically coupled to primary side V_M is:

$$V_M = \frac{V_I}{\omega L_1} \times \omega M_1 = \frac{V_I M_1}{L_1}. \tag{18}$$

The input current of relay circuit I_{M1} is:

$$I_{M1} = \frac{V_M}{R_{ML}}. \tag{19}$$

The current of relay circuit I_{M2} is:

$$I_{M2} = \frac{I_{M1}(\omega L_2)^2 R_{SL}}{wL_2[(\omega M_2)^2 + R_{SL}R_3]}. \tag{20}$$

The induced voltage of pickup coil V_P is:

$$V_P = \omega M_2 I_{M2}. \tag{21}$$

The input current of pickup I_{S1} is:

$$I_{S1} = \frac{V_P}{R_{SL}}. \tag{22}$$

The output current of pickup I_{S2} is:

$$I_{S2} = \frac{V_P}{R_{SL}} \times \frac{(\omega L_3)^2}{R_L} \times \frac{1}{\omega L_3}. \tag{23}$$

The output power of system P_{out} is:

$$P_{out} = \left(\frac{|V_I| M_1 M_2 \omega^3 L_2 L_3}{L_1 R_2 \left[R_3 R_4 R_L + R_3 (\omega L_3)^2 + R_L (\omega M_2)^2 \right] + (\omega L_2)^2 [R_4 R_L + (\omega L_3)^2]} \right)^2 R_L. \tag{24}$$

From Eq. (24), for a given load R_L, the output power of the system is proportional to mutual inductance M_1 and the module of primary output voltage $|V_I|$.

If

$$\frac{dP_{out}}{dM_2} = 0, \tag{25}$$

then

$$M_{2-power} = \frac{1}{\omega} \sqrt{\frac{R_2 R_3 R_4 R_L + R_2 R_3 (\omega L_3)^2 + (\omega L_2)^2 [R_4 R_L + (\omega L_3)^2]}{R_2 R_L}}. \tag{26}$$

Under the condition of Eq. (26), the maximum output power of the system is:

$$P_{out\max} = \frac{\left(|V_I| M_1 \omega^2 L_2 L_3 \right)^2}{4 L_1^2 R_2 \left[R_2 R_3 R_4 R_L + R_2 R_3 (\omega L_3)^2 + (\omega L_2)^2 (R_4 R_L + (\omega L_3)^2) \right]}. \tag{27}$$

Due to the limitation of $M_2 < \min(L_{M2}, L_{S1})$, an optimal parameter may not exist in the actual system. The input resistance of primary R_{PL} is:

$$R_{PL} = \frac{(\omega L_1)^2}{R_1 + R_{eq}}. \tag{28}$$

The input power of the system is:

$$P_{in} = \frac{|V_I|^2}{R_{PL}}. \tag{29}$$

Efficiency η of the system can be calculated as:

$$\eta = \frac{\omega^6 M_1^2 M_2^2 L_2^2 L_3^2 R_L R_{PL}}{L_1^2 \left[R_2 \left[R_3 R_4 R_L + R_3(\omega L_3)^2 + R_L(\omega M_2)^2\right] + (\omega L_2)^2 \left[R_4 R_L + (\omega L_3)^2\right]\right]^2}, \tag{30}$$

and if

$$\frac{d\eta}{dM_2} = 0, \tag{31}$$

then

$$M_{2-efficiency} = f\left(\omega, R_1, R_2, R_3, L_1, L_2, L_3, M_1\right). \tag{32}$$

Eq. (31) can be simplified by representing it with Eq. (32), which is an optimal parameter of the system.

6. Results of the experiment

To verify the viability of the proposed relay WPT system, an experimental system is set up. Since the proposed system is completely symmetrical in structure and parameters, only the energy from the primary to the pickup is studied while the opposite mode is the same as energy from the primary to the pickup side. In Figure 3, the full bridge reversible rectifier, which can be controlled by a PWM shift phase strategy, is operated in inverting mode or rectifying mode, depending on the direction of the power flow, where the power switch of the full bridge uses MOSFET, all resonant inductance of system is 134.8 μH, all compensation capacitance is 0.47 μF, and the DC voltage of the primary side is 30 V. Based on Figure 5, the output of the pickup circuit is connected to load R_Z, which is 45 Ω, and filter capacitor C_Z is 100 μF. The primary and pickup control circuit comprises two parts: a microprocessor and a driving circuit. The microprocessor is DSP (TMS320F28335) to generate a shift phase pulse while the driving circuit is composed of integrated driving chip IR2110. A photograph of the experimental set up is given in Figure 11.

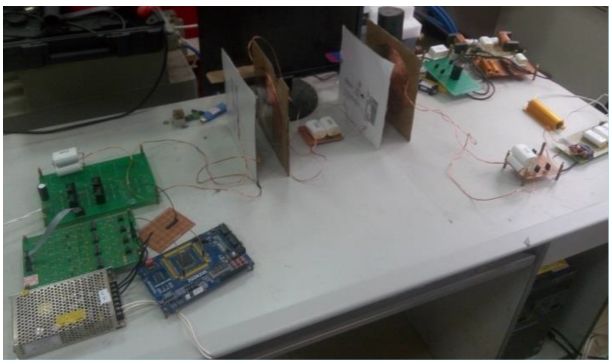

Figure 11. Photograph of the experimental set up.

6.1. Verification of frequency stability characteristic

Figures 12a–12d are the waveforms of the output current I_{P1} and output voltage of the primary power converter V_I, where the primary phase shift angle ϕ and the pickup phase shift angle λ take $(\pi/4, 0)$, $(\pi/4, \pi/4)$, $(0, \pi/4)$, and $(0, 0)$, respectively.

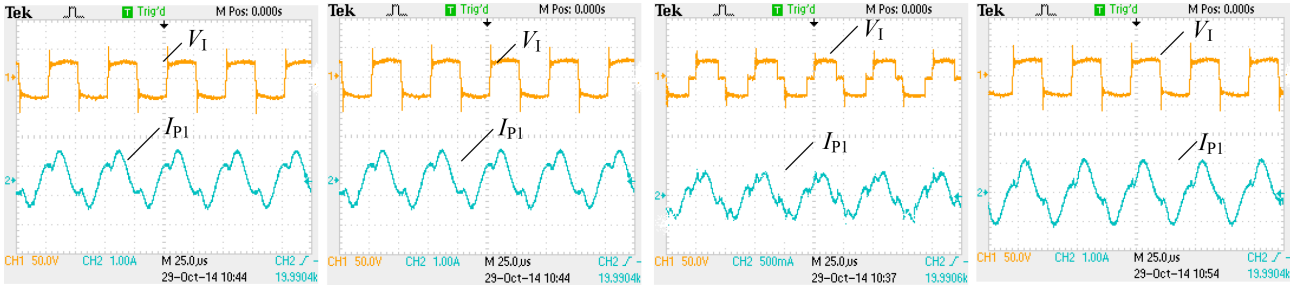

Figure 12. The waveform of the frequency stability characteristic: a) $\phi = \pi/4$, $\lambda = 0$, b) $\phi = \pi/4$, $\lambda = \pi/4$, c) $\phi = 0$, $\lambda = \pi/4$, d) $\phi = 0$, $\lambda = 0$.

From Figure 12, under a different shift phase control, the phase angle of the primary inverter output voltage and the primary inverter output current is almost the same, which is not affected by the primary and pickup phase angle.

6.2. Verification of primary constant current characteristic

Figures 13a–13d are the waveforms of current I_{P2} flowing from primary coil L_{P2} and the output voltage of primary power converter V_I when the primary side shift phase angle ϕ and the pickup shift phase angle λ take $(\pi/4, 0)$, $(\pi/4, \pi/4)$, $(0, \pi/4)$, and $(0, 0)$, respectively, aiming to verify that the LCL resonant compensation circuit can hold the current of the primary coil constant.

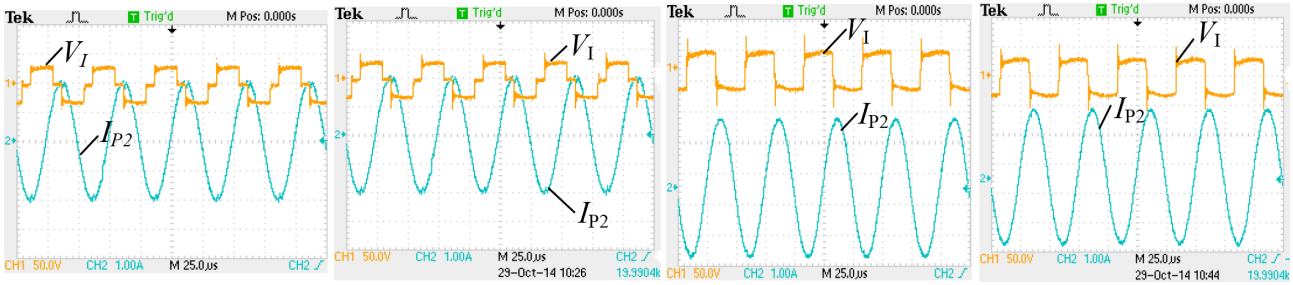

Figure 13. The waveform of the primary coil current: a) $\phi = \pi/4$, $\lambda = 0$, b) $\phi = \pi/4$, $\lambda = \pi/4$, c) $\phi = 0$, $\lambda = \pi/4$, d) $\phi = 0$, $\lambda = 0$.

As seen from Figure 13, for a given primary inductance, the primary coil current only depends on the output voltage of the primary inverter while it is unrelated to the shift phase of pickup. The equivalent load of pickup varies with the pickup side shift phase angle, which proves that the primary coil current is unrelated to the load indirectly.

6.3. Verification of power control strategy

Figures 14a–14d are the waveforms of the pickup side rectifier output voltage and input current I_{S2} when the primary phase shift angle ϕ and the secondary phase shift angle λ take $(\pi/4, 0)$, $(\pi/4, \pi/4)$, $(0, \pi/4)$, and $(0, 0)$, respectively.

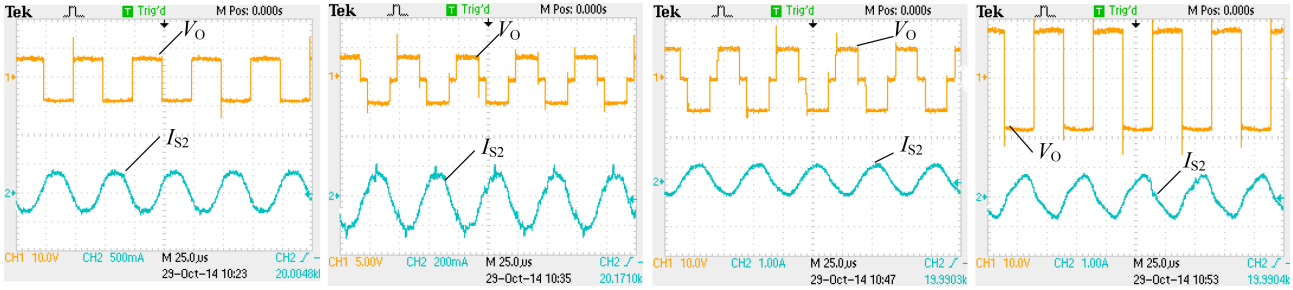

Figure 14. The waveform of the power control strategy: a) $\phi = \pi/4$, $\lambda = 0$, b) $\phi = \pi/4$, $\lambda = \pi/4$, c) $\phi = 0$, $\lambda = \pi/4$, d) $\phi = 0$, $\lambda = 0$.

From Figure 14, the received power of the pickup side varies with the primary side and the pickup side shift phase angle, which increases with the shift phase angle.

6.4. Verification of bidirectional transfer characteristic

To verify the direction in which power flow can be controlled, the output of pickup circuits is connected to individual DC sources. The control block algorithm for bidirectional power flow is given in Figure 15.

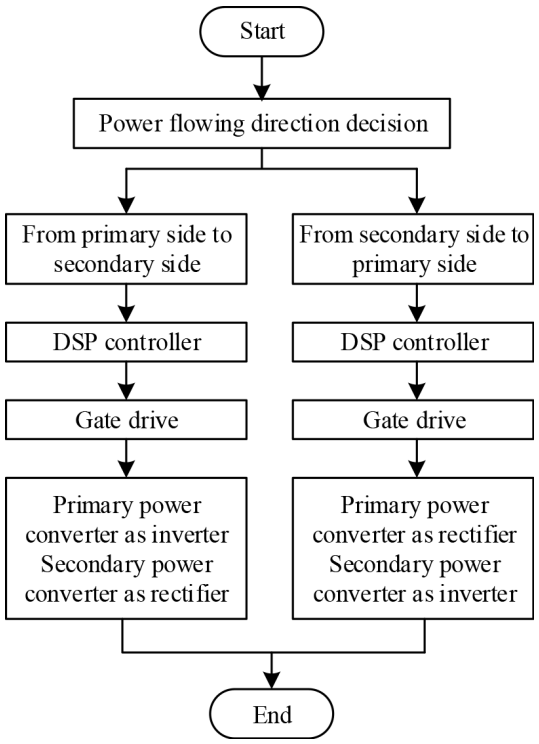

Figure 15. The control block algorithm for bidirectional power flow.

The primary DC voltage is 30 V while the pickup side DC source is 45 V and the other system parameters are consistent with the above.

Figure 16 shows the experimental waveform of the primary power converter and pickup power conditioner output voltage when relative initial phase α is $-\pi/2$.

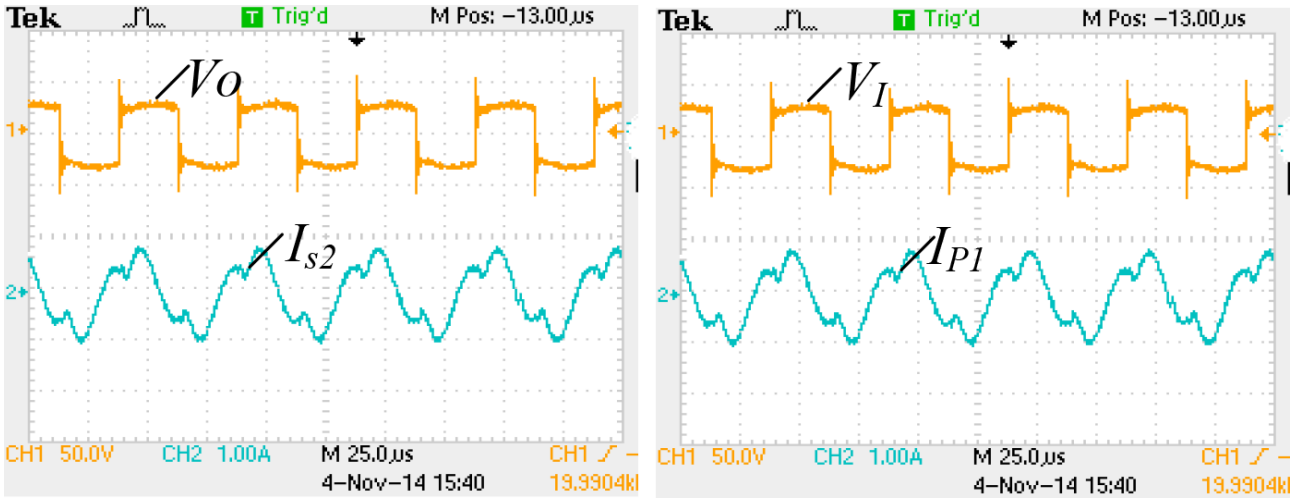

Figure 16. The waveform of the output current of the primary and pickup side when $\alpha = -\pi/2$.

Figure 16a is the waveform of pickup power conditioner output voltage V_0 and output current I_{s2} and Figure 16b is the waveform of primary power converter output voltage V_I and output current I_{P1}. From Figure 17, the pickup received power is positive and the primary input power is also positive, which indicates that the direction of power flow is from the primary to the pickup side.

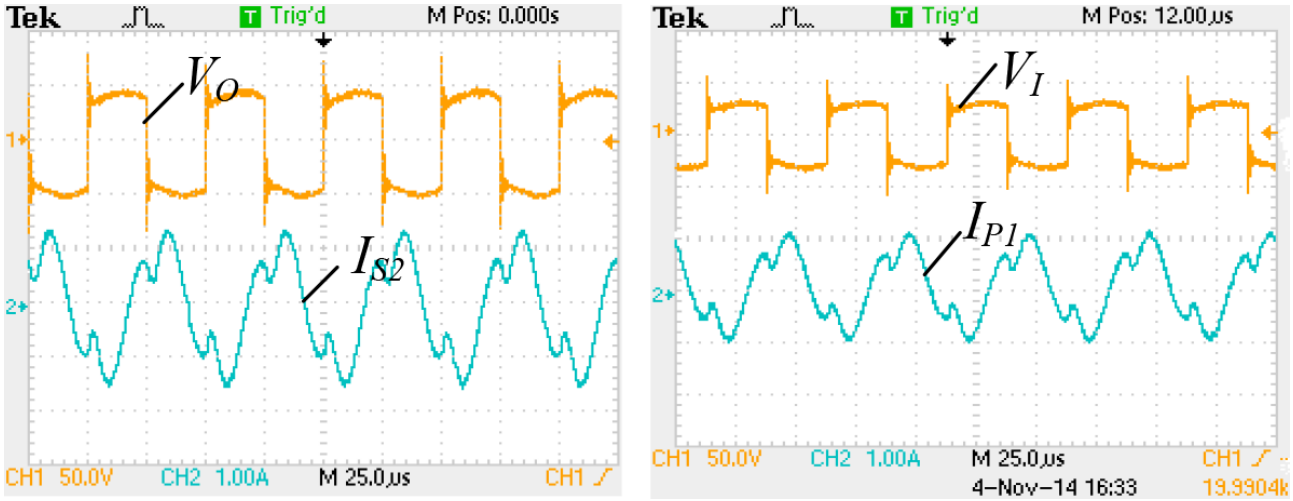

Figure 17. The waveform of the output current of the primary and pickup side when $\alpha = \pi/2$.

Figure 17 is the waveform of the primary power converter and pickup power conditioner output voltage when relative initial phase α is $\pi/2$.

Figure 17a shows the waveform of pickup power conditioner output voltage V_0 and output current I_{s2}. Figure 17b is the waveform of the primary power converter output voltage V_I and output current I_{p1}. From Figure 17, the pickup received power is negative and the primary input power is also negative, which indicates that the direction of power flow is from the pickup to the primary.

6.5. Verification of transfer power and parameter optimization of the system

In order to compare the efficiency and power flow with the existing topology, we set up a WPT system with a relay circuit and one without a relay circuit. The efficiency and power flow are measured while changing the positions of the primary and secondary coils (the mutual inductance of the primary and secondary self-inductances) in these two systems. The results are shown in Figure 18.

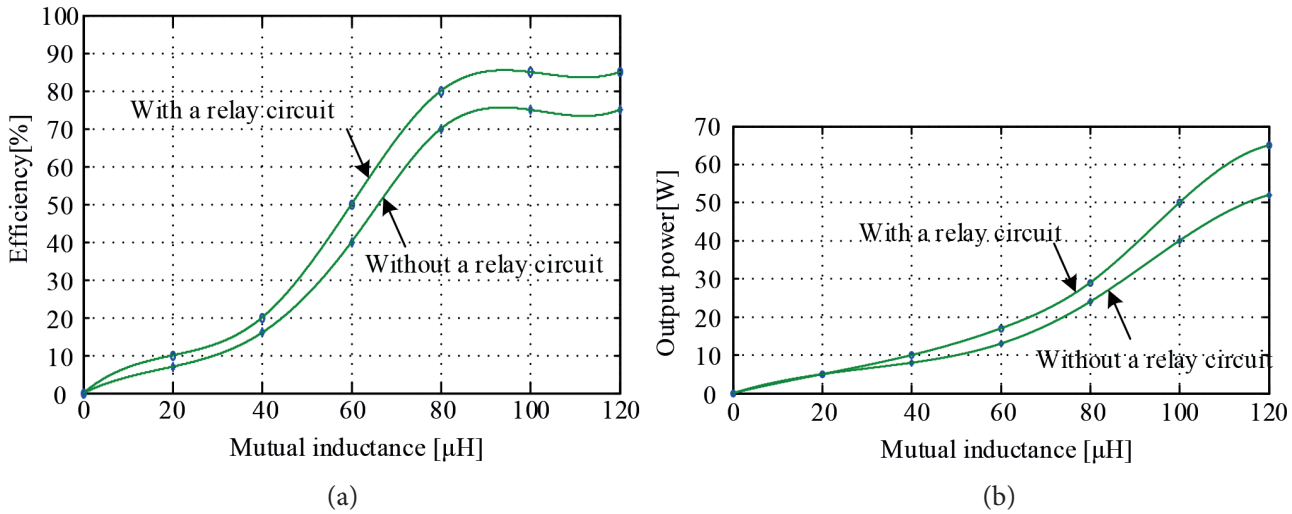

Figure 18. Comparison of the efficiency and output power with or without a relay circuit: a) efficiency curve, b) output power curve.

7. Conclusion

This paper proposes a new relay bidirectional WPT system based on LCL topology to resolve the contradictions between transfer distance, coil misalignment, and efficiency. The proposed system is analyzed in terms of structure feature, parameter design and optimization, and its working modules. These theoretical analyses are verified by practical experiments and the good performance of this system can make it applicable in EV charging systems.

Acknowledgment

This work was supported by the Fundamental Research Funds for the Central Universities (China University of Mining and Technology) under Grant 2014ZDPY17.

References

[1] Elliott GAJ, Raabe S, Covic GA, Boys JT. Multiphase pickups for large lateral tolerance contactless power transfer systems. IEEE T Ind Electron 2010; 57: 1590-1598.

[2] Liu X, Hui SY. Optimal design of a hybrid winding structure for planar contactless battery charging platform. IEEE T Power Electr 2008; 23: 455-463.

[3] Madawala UK, Thrimawithana DJ. Current sourced bi-directional inductive power transfer system. IET Power Electron 2011; 4: 471-480.

[4] Sun Y, Tang C, Hu AP, Li HL, Nguang SK. Multiple soft-switching operating points-based power flow control of contactless power transfer systems. IET Power Electron 2011; 4: 725-731.

[5] Egan MG, O'Sullivan DL, Hayes JG, Willers MJ, Henze CP. Power factor corrected single stage inductive charger for electric vehicle batteries. IEEE T Ind Electron 2007; 54: 1217-1226.

[6] Si P, Hu AP, Malpas S, Budgett D. A frequency control method for regulating wireless power to implantable devices. IEEE T Biomed Circ S 2008; 2: 22-29.

[7] Wu HH, Hu AP, Si P, Tung C, Budgett D, Malpas S. A push-pull resonant converter with dual coils for transcutaneous energy transfer systems. In: 2009 4th IEEE Conference on Industrial Electronics and Applications; 25–27 May 2009; Xian, China. New York, NY, USA: IEEE. pp. 1051-1056.

[8] Madawala UK, Thrimawithana DJ, Kularatna N. An ICPT supercapacitor based hybrid system for surge free power transfer. IEEE T Ind Electron 2007; 54: 3287-3297.

[9] Zhang Y, Zhao Z, Lu T. Quantitative analysis of system efficiency and output power of four-coil resonant wireless power transfer. IEEE J Em Sel Top P 2015; 3:184-190.

[10] Villa JL, Sallan J, Osorio JFS, Llombart A. High-misalignment tolerant compensation topology for ICPT systems. IEEE T Ind Electron 2012; 59: 945-951.

[11] Sallán J, Villa JL, Llombart A, Sanz JF. Optimal design of ICPT systems applied to electric vehicle battery charge. IEEE T Ind Electron 2009; 56: 2140-2149.

[12] Zhong WX, Lee CK, Hui SY. Wireless power domino-resonator systems with noncoaxial axes and circular structures. IEEE T Power Electr 2012; 27: 4750-4762.

[13] Madawala UK, Thrimawithana DJ. A two-way inductive power transfer interface for single loads. In: 2010 IEEE International Conference on Industrial Technology; 14–17 March 2010; Valparaiso, Chile. New York, NY, USA: IEEE. pp. 673-678.

[14] Thrimawithana DJ, Madawala UK. A contactless bidirectional power interface for plug-in hybrid vehicles. In: 2009 IEEE Vehicle Power and Propulsion Conference; 7–10 September 2009; Dearborn, MI, USA. New York, NY, USA: IEEE. pp. 396-401.

[15] Thrimawithana DJ, Madawala UK. A three-phase bi-directional IPT system for contactless charging of electric vehicles. In: 2011 IEEE International Symposium on Industrial Electronics; 27–30 June 2011; Penang, Malaysia. New York, NY, USA: IEEE. pp. 1957-1962.

[16] Hu C, Sun Y. Optimal design of electromagnetic coupling mechanism for ICPT system. In: 2013 IEEE 8th Conference on Industrial Electronics and Applications; 19–21 June 2013; Melbourne, Australia. New York, NY, USA: IEEE. pp. 1233-1237.

[17] Wang C, Covic GA. Investigating an LCL Load resonant inverter for inductive power transfer applications. IEEE T Power Electr 2004; 19: 995-1002.